PRZEGLĄD ELEKTROTECHNICZNY

OPEN ACCESS

Szymon RACEWICZ
ORCID: 0000-0002-3426-9767
DOI: 10.15199/48.2025.11.6

Sensitivity analysis of synchronous generator non-integer order model parameters for SSFR identification

Analiza wrażliwości parametrów modelu rzędu niecałkowitego generatora synchronicznego do celów identyfikacji metodą SSFR

dr inż. Szymon Racewicz, Uniwersytet Warmińsko-Mazurski w Olsztynie, Katedra Mechatroniki, ul. Oczapowskiego 11, 10-719 Olsztyn
Correspondence address: szymon.racewicz@uwm.edu.pl

Abstract: This paper presents a sensitivity analysis of the synchronous generator non-integer order model parameters for SSFR (Standstill Frequency Response) identification. The equivalent circuits of the generator, comprising 10 parameters in the d-axis and 7 parameters in the q-axis, were prepared for a 3 kVA and a 125 kVA synchronous machines. Then, an analysis of the model fitting errors to the measured SSFR characteristics was performed for the changing with saturation selected parameters of the non-integer order model.

Keywords: non-integer order modelling, synchronous generator, equivalent circuit, parameter identification, SSFR

Streszczenie: Artykuł przedstawia analizę wrażliwości parametrów modelu rzędu niecałkowitego generatora synchronicznego do celów identyfikacji metodą SSFR (StandStill Frequency Response). Obwodowy schemat zastępczy generatora zawierający 10 parametrów w osi d oraz 7 parametrów w osi q został przygotowany dla maszyn synchronicznych o mocy 3 kVA i 125 kVA. Następnie przeprowadzono analizę błędów dopasowania modeli do zmierzonych charakterystyk SSFR dla zmieniających się wraz z nasyceniem wybranych parametrów modelu rzędu niecałkowitego.

Słowa kluczowe: modelowanie rzędu niecałkowitego, generator synchroniczny, schemat zastępczy, identyfikacja parametrów, SSFR

Introduction

In modern power systems, synchronous generators (SG) remain the primary source of electrical energy. Given the ever-increasing number of components, as well as the desire for more accurate predictions of behaviours and interactions among the various electrical elements of such networks, it is crucial to continuously improve the mathematical models of different components of the power system [1], [2], [3], [4]. The application of SG is not limited to providing power to large, stationary power networks. Such machines are also present in Combined Heat and Power (CHP) units or the onboard electrical systems of modern aeroplanes and ships. Therefore, their range of applications, construction, and operating conditions is vast. To accurately model the operation of a synchronous machine, many factors must be considered, including phenomena related to the operating frequency of such machines [5], [6], [7]. These phenomena include the skin effect that appears in some conductive parts of the generator, such as damper cage bars, and eddy currents that occur in solid steel parts of the machine, such as pole shoes or the rotor shaft [8]. Magnetic saturation is also a key factor for accurate modelling of such machines. Therefore, literature contains numerous references to the construction, operation, and various models of SG, ranging from simple to complex [9], [10], [11]. Accuracy of the model used further implies the accuracy of the entire system, e.g. the so-called "Digital Twin" or the Power Hardware In the Loop (PHIL) platform, which have been increasingly developed in recent years [12], [13].

One of the most original mathematical models of synchronous machines is based on fractional-order derivatives (FOD) [14], [15]. For centuries, fractional calculus remained primarily a theoretical tool used by mathematicians. It was not until the advent of computers and the development of computational techniques, combined with formal mathematical notation, that non-integer order calculus could be effective-

ly applied to model and analyse real-world systems. Non-integer order modelling is particularly useful in systems where physical phenomena such as diffusion (electromagnetic fields, temperature, gases, fluids), energy and heat exchange, proton exchange, electrochemical reactions, frequency-related effects (skin effect, eddy currents), etc., are present. One of the main advantages of the non-integer order models includes a reduced number of parameters compared to classical integer-order ones and greater accuracy, especially in the frequency domain [16]. This property stems from the model's reduced order while achieving a more precise mathematical description of the physical phenomenon. As a result, non-integer order modelling finds applications in behavioural models of devices and systems such as batteries [17], super and ultracapacitors [18], fuel cells [19], electric machines [20], and even automotive suspensions [21]. Furthermore, it is also increasingly used in control theory [22].

Nevertheless, aside from the adopted compact model structure, accurate modelling of electric components also requires an effective parameter identification method.

There are many methods for parameter identification of equivalent circuits. In general, they can be divided into time-domain and frequency-domain methods. The latter are advantageous for systems where frequency characteristics are more prominent, which is the case of SG. The StandStill Frequency Response (SSFR) test [23] is used to validate a model for a wide frequency range, which enables studying the earlier-mentioned phenomena related to the operating frequency of the tested machine. Combined with the optimised least-squares method algorithm, it enables a global identification of all the model parameters at once. However, this process may be ineffective when the parameters being identified affect the model output in the same frequency ranges. Then, the mathematical optimisation algorithm cannot correctly distinguish the direct contribution of each parameter to the model output, which may lead to the loss of the physical meaning of these parameters. It is then crucial to study the model parameters' influence on the variability of frequency characteristics curves to correctly design the identification process.

The paper is organised as follows. First, the equivalent circuits of the non-integer order model of SG in the d-q reference frame are recalled. Second, the SSFR characteristics of two saturated synchronous machines of 3 kVA and 125 kVA are presented. Then, a sensitivity analysis of the selected model parameters for the determined frequency ranges is performed. Finally, the conclusions are formulated.

The main contributions of the paper are as follows:

- Presentation of the non-integer order model of SGs of 3 kVA and 125 kVA.
- Comparison of the SSFR characteristics of both 3 kVA and 125 kVA SGs in saturated conditions.
- Performing the sensitivity analysis of SG non-integer order model parameters for the low and high frequency range.

Non-integer order model of SG

The starting point for the research was the development of the non-integer order mathematical model of SG in the d and q axes (Fig. 1).

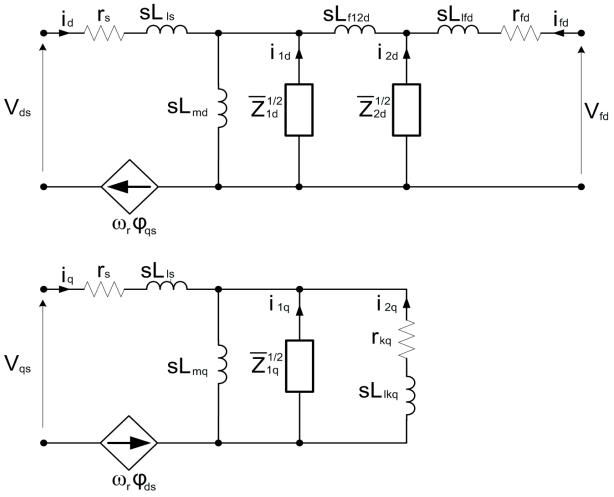

Fig. 1. Non-integer order equivalent circuits of SG (axes d and q).

The above model has been widely described in publications, including [24], [25]. It contains 10 parameters in the d-axis and 7 parameters in the q-axis to evaluate or identify. The half-order impedances in *explicit* form are given by the equations (1), (2) and (3). They replace the R-L ladder networks with lumped parameters in the classical model [26].

$$\overline{Z}_{1d}^{1/2}(s)=\frac{L_{1d}\cdot s}{1+\sqrt{\frac{s}{\omega_{1d}}}} \tag{1}$$

$$\overline{Z}_{1q}^{1/2}(s)=\frac{L_{1q}\cdot s}{1+\sqrt{\frac{s}{\omega_{1q}}}} \tag{2}$$

$$\overline{Z}_{2d}^{1/2}(s)=R_{2d}\cdot\left(1+\sqrt{\frac{s}{\omega_{2d}}}\right) \tag{3}$$

where:

L_{1d}, L_{1q} – DC inductances of the modelled massive parts of the rotor,

R_{2d} – DC resistance of the modelled damper bars,
ω_{1d}, ω_{1q}, ω_{2d} – cut-off pulsations [27].

Finally, the complete model consists of the following variables and parameters: V_{ds} and V_{qs} are the armature voltages in the d and q axes, V_{fd} is the excitation voltage, i_{ds} and i_{qs} are the armature currents in the d and q axes, i_{fd} is the excitation current, i_{1d} and i_{1q} are the currents passing through the non-integer order inductive type impedances (1) and (2), respectively in the d and q axes, i_{2d} and i_{2q} are the currents passing through the resistive type impedance (3) and the classic R-L branch, respectively in the d and q axes. Next, r_s and r_{fd} are the resistances of the stator and field windings, respectively; L_{md} and L_{mq} are the magnetising mutual inductances of the machine in the d and q axes, L_{ls} and L_{lfd} are the leakage inductances of armature windings and field winding, respectively, and L_{f12d} is the mutual inductance linking field and damper windings. The model, written as a system of equations, is presented by formula (4):

$$(4)\quad \begin{cases} V_{ds} = r_s \cdot i_{ds} - \omega_r \varphi_{qs} + s \cdot \varphi_{ds} \\ V_{qs} = r_s \cdot i_{qs} + \omega_r \varphi_{ds} + s \cdot \varphi_{qs} \\ 0 = Z_{1d}^{1/2} \cdot i_{1d} + s \cdot \varphi_{1d} \\ 0 = Z_{2d}^{1/2} \cdot i_{2d} + s \cdot \varphi_{2d} \\ 0 = Z_{1q}^{1/2} \cdot i_{1q} + s \cdot \varphi_{1q} \\ 0 = r_{kq} \cdot i_{2q} + s \cdot \varphi_{2q} + s \cdot \varphi_{1q} \\ V_{fd} = r_{fd} \cdot i_{fd} + s \cdot \varphi_{fd} \end{cases}$$

where the flux components are given by (5), (6), (7), (8), (9), (10) and (11):

$$(5)\quad \varphi_{ds} = L_{ls} \cdot i_{ds} + L_{md}\left(i_{ds} + i_{1d} + i_{2d} + i_{fd}\right)$$

$$(6)\quad \varphi_{qs} = L_{ls} \cdot i_{qs} + L_{mq}\left(i_{qs} + i_{1q} + i_{2q}\right)$$

$$(7)\quad \varphi_{1d} = L_{md}\left(i_{ds} + i_{1d} + i_{2d} + i_{fd}\right)$$

$$(8)\quad \varphi_{1q} = L_{mq}\left(i_{qs} + i_{1q} + i_{2q}\right)$$

$$(9)\quad \varphi_{2d} = \varphi_{1d} + L_{f12d}\left(i_{2d} + i_{fd}\right)$$

$$(10)\quad \varphi_{2q} = L_{lkq} \cdot i_{2q}$$

$$(11)\quad \varphi_{fd} = \varphi_{2d} + L_{lfd} \cdot i_{fd}$$

Some of the parameters, i.e. r_s and r_{fd} or L_{1d}, L_{1q}, L_{md}, L_{mq}, and L_{ls}, can be directly evaluated based on measurements or technical data provided by the machine supplier, whereas the other (ω_{1d}, ω_{1q}, R_{2d}, ω_{2d}, r_{kq}, L_{lkq}, L_{f12d}, L_{lfd}) need to be identified [27]. For this article, we assume that the variability of the SSFR frequency characteristics with saturation will be most visible in the d-axis due to the salient rotor construction of the tested machines. Therefore, the values in p.u. of all the parameters only in the d-axis are presented in Table 1 for both machines. The rated quantities of the studied machines as well as their base values, are presented in the appendix.

Table 1. SGs model parameters in d-axis

Parameter	Enco 3 kVA [p.u.]	Elmor 125 kVA [p.u.]
r_s	0.0537	0.0261
L_{ls}	0.0880	0.0962
L_{md}	1.5399	1.0271
L_{1d}	6.9862	2.6960
ω_{1d}	0.0044	0.0126
L_{f12d}	0.0163	0.0147
R_{2d}	0.0378	0.0095
ω_{2d}	0.1285	0.0432
L_{lfd}	0.0102	0.2202
r_{fd}	0.0372	0.0067

Fig. 2 shows the operational characteristics of the two SGs, i.e. no-load characteristic and short-circuit characteristic, which reflect the machines' behaviour under different operating conditions.

SSFR characteristics measurement

To study the variability of synchronous machine SSFR characteristics with saturation, the measurement setup presented in Fig. 3 was developed.

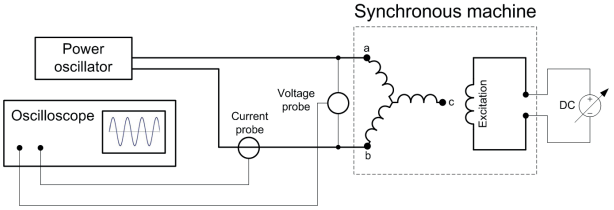

Fig. 3. Measurement setup for SSFR characteristics of a saturated synchronous machine.

In contrast to the classical SSFR method used for linear conditions, a field winding is short-circuited by a controlled DC voltage source, which enables an injection of the magnetising current during the regular SSFR tests. Such tests were performed on two

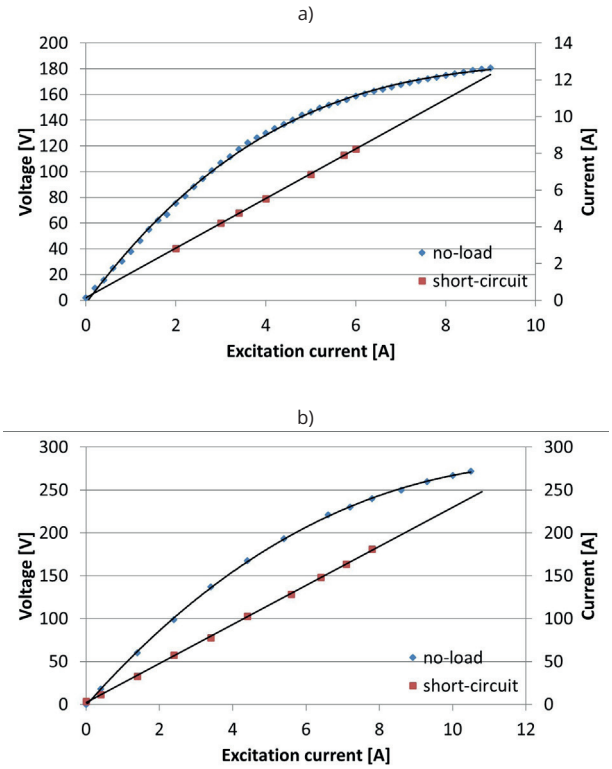

Fig. 2. No-load and short-circuit characteristics of 3 kVA (a) and 125 kVA (b) SGs.

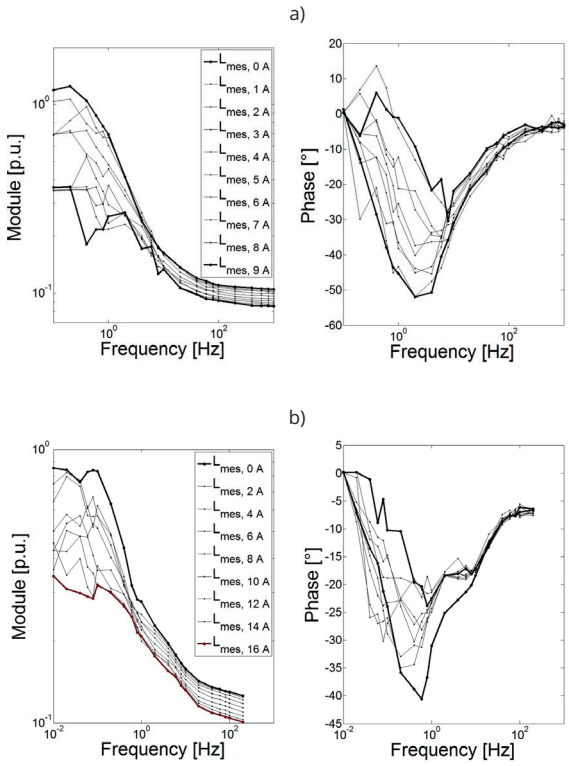

Fig. 4. Operational inductance L_d of 3 kVA (a) and 125 kVA (b) SGs for different magnetising currents.

salient rotor SGs of 3 kVA and 125 kVA. The magnetising current was changed in the range of 0–9 A and 0–16 A for the 3 kVA and the 125 kVA machine, respectively. For each magnetising current, the SSFR test was performed in the range of 0.1–1 kHz for the 3 kVA SG and in the range of 0.01–200 Hz for the 125 kVA SG. The operational inductance L_d given by (12) along the d-axis, where the influence of saturation is the most pronounced due to the smaller air gap, is shown in Fig. 4 for the 3 kVA (a) and the 125 kVA (b) machines, respectively.

$$\overline{L}_d = \frac{\overline{Z}_d - r_s}{j\omega} \tag{12}$$

where:
Z_d – measured impedance,
r_s – armature resistance,
ω – pulsation.

The extreme lines have been bolded to better show the variation of the operational inductance over the magnetising current range. The lines in between are drawn in the same style to show only the area of operational inductance variation.

Analysing Fig. 4, one can find that the variability of the SSFR characteristics with saturation, especially for the module, is observed in the whole frequency range for both machines of different powers. This implies the need for further analysis regarding the influence of specific model parameters on the model output response in specific frequency ranges. This analysis helps to better understand and design the model parameters identification process based on the SSFR method.

Sensitivity analysis

As shown in the previous chapter, magnetic saturation influences the SSFR characteristics of SG in the whole frequency range. While analysing the d-axis equivalent circuit of the machine (Fig. 1), we can state that for low frequencies, there are three inductances, namely L_{ls}, L_{md} and L_{1d}, which can be affected by the saturation. At high frequencies, however, the saturation effect can affect the L_{ls} and the other two inductances, namely L_{fl2d} and L_{1fd}. Unfortunately, since we have only one operational inductance L_d from the SSFR test, we are unable to precisely differentiate the influence of saturation on each inductance. Having this in mind, the sensitivity analysis of the above-mentioned non-integer order model parameters was performed for 3 kVA and 125 kVA SGs.

Fig. 5 and Fig. 6 show the percentage relative error of the model output at low and high frequencies, respectively, for the percentage variation of the above-discussed inductances for unsaturated conditions. For both machines, the low frequency range was the first frequency decade of the SSFR measurements, while the high frequency range was the last frequency dec-

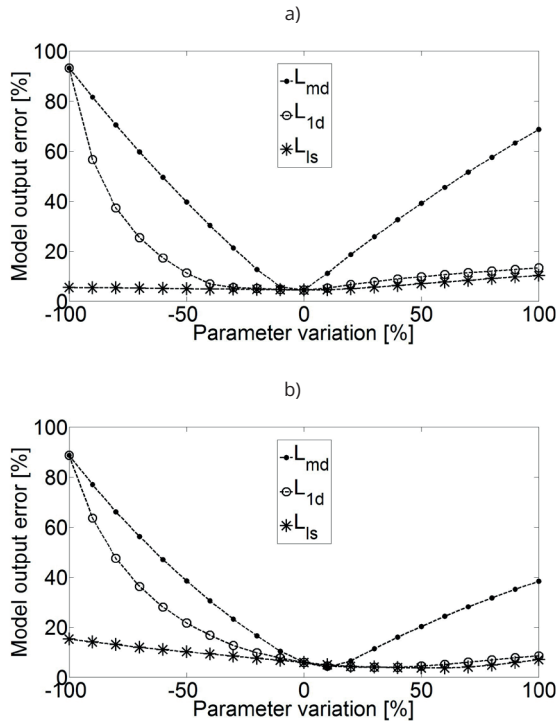

Fig. 5. Model output error at low frequencies to the variation of the inductances L_{md}, L_{1d} and L_{ls} for 3 kVA (a) and 125 kVA (b) SGs.

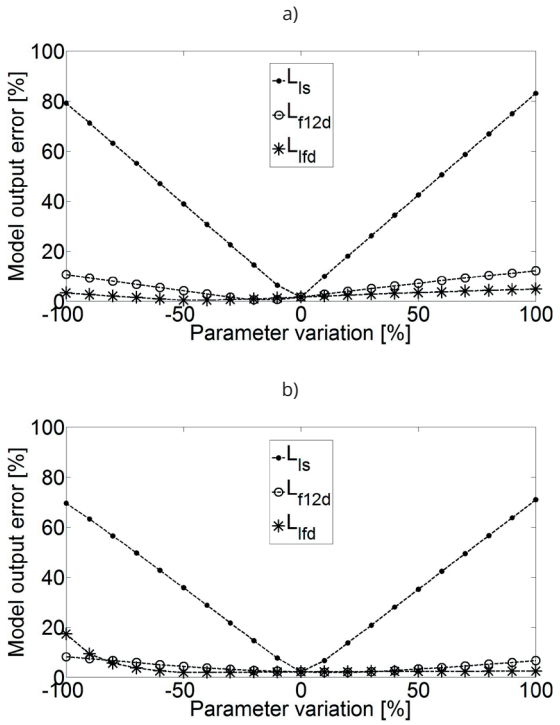

Fig. 6. Model output error at high frequencies to the variation of the inductances L_{ls}, L_{f12d} and L_{lfd} for 3 kVA (a) and 125 kVA (b) SGs.

ade. Each inductance was varied within the range (-100%, +100%) of the p.u. value, while the rest of the parameters were kept constant. Then, the average percentage relative error between the measurement and the simulation was calculated for the previously determined frequency range.

From the figures above (Fig. 5 and Fig. 6) for both machines, it appears that at low frequency range, the main magnetising inductance L_{md} is the most susceptible to saturation changes, whereas at high frequencies, it is the L_{ls} leakage inductance. The remaining inductances are also affected by saturation to some extent, but as mentioned earlier, the lack of information from the SSFR procedure prevents a quantitative assessment of this effect. Therefore, to take into account the saturation effect in the non-integer order model of SG, it is recommended to assume the variation of the L_{md} magnetising inductance for low frequencies and the L_{ls} leakage inductance for high frequencies, while the rest of the parameters should be kept constant with the magnetising current.

Conclusion

The presented research showed the variability of the selected parameters of the non-integer order model of SG under magnetic saturation. This analysis can be used for designing the identification process based on the SSFR method. It involves the proper selection of model parameters whose variability is most significant for the modelled phenomenon. Then, the global identification process can be run, but with fewer degrees of freedom, which increases the overall efficiency and accuracy of the identification process. SSFR is performed at a standstill, eliminating the need for the machine to operate under load or dynamic conditions, as required by classical tests. This makes SSFR less invasive and more practical for industrial applications. Moreover, SSFR facilitates parameter identification across a broad frequency spectrum, crucial for modelling complex dynamic phenomena. Unlike classical methods, such as short-circuit or load tests, SSFR accounts for nonlinearities like magnetic saturation, which significantly affect machine parameters. In combination with a non-integer order model, which captures systems with memory and nonlinearities more effectively than classical integer-order ones, the presented approach enables better representation of complex phenomena, such as magnetic saturation or core losses.

Continuous development and refinement of different parameter identification methods contribute to a better understanding and deeper analysis of the potential application of mathematical models. The two-axis circuit model (Clarke-Park) of SG, based on the theory of non-integer order derivatives, demonstrates greater accuracy in many areas compared to the classical one. It is then essential to study its suitability and adaptability for modelling the phenomena occurring in SGs more and more accurately. The combination of

SSFR testing and non-integer order modelling opens new research areas for more accurate and comprehensive SG parameter identification.

Appendix

Enco and Elmor GCh114o/4 SGs base values:

Parameter	Enco	Elmor
Base frequency	50 Hz	50 Hz
Base pulsation	314.16 rad/s	314.16 rad/s
Base impedance	16.13 kΩ	1.28 Ω
Base inductance	0.0514 H	0.0041 H

Enco and Elmor GCh114o/4 SGs rated data:

Parameter	Enco	Elmor
Apparent power	3 kVA	125 kVA
Stator voltage	220 V	400 V
Stator current	7.9 A	180 A
Rotor voltage	20 V	99 V
Rotor current	8 A	17.4 A
Frequency	50 Hz	50 Hz
Rotational speed	1500 rpm	1500 rpm
Power factor	0.8	0.8

Received: 19.10.2025, **Accepted:** 05.11.2025, **Published:** 24.11.2025

REFERENCES

[1] Modi N. et al., Model Acceptance Testing, (2024), Springer Nature Link, 2024, 711–743. doi: 10.1007/978-3-031-47821-5_15.

[2] Wu X., Cao B., Xing Y., Shen Z., Research on simulation accuracy of equivalent aggregate electromagnetic model optimization for large renewable energy stations, J. Phys. Conf. Ser., 2797 (2024), No. 1, 012039, doi: 10.1088/1742-6596/2797/1/012039.

[3] Agrawal B., Kosterev D., Model Validation Studies for a Disturbance Event That Occurred on June 14 2004 in the Western Interconnection, in 2007 IEEE Power Engineering Society General Meeting, IEEE, Jun. 2007, 1–5. doi: 10.1109/PES.2007.386212.

[4] Boumous S., Boumous Z., Djeghader Y., Boumous M., New approach to power system stabilizer optimization techniques, Diagnostyka, 25 (2024), No. 4, 1–8, doi: 10.29354/diag/194669.

[5] Quadri Q. H., Nuzzo S., Gerada C., Galea M., Analysis and Modelling of High Frequency Effects on Synchronous Generator's Armature Conductors, in 2020 IEEE 29th International Symposium on Industrial Electronics (ISIE), IEEE, Jun. 2020, 253–258. doi: 10.1109/ISIE45063.2020.9152456.

[6] Plötz S., Ranzinger L., Uhrig S., Frequency Response Analysis on Rotating Machines – Model Parameterization for Different Machine Types and Performance Classes, in 2024 International Conference on Diagnostics in Electrical Engineering (Diagnostika), IEEE, Sep. 2024, 01–06. doi: 10.1109/Diagnostika61830.2024.10693894.

[7] Alberti L., Bottesi O., Bolognani S., Computation and measurement of high frequency parameters in a synchronous machine, in 2015 IEEE Energy Conversion Congress and Exposition (ECCE), IEEE, Sep. 2015, 845–852. doi: 10.1109/ECCE.2015.7309776.

[8] Benmebarek F., Three-Dimensional Numerical Modelling of Eddy Current System Using the Finite Volume Method, PRZEGLĄD ELEKTROTECHNICZNY, 1 (2024), No. 2, 129–133, doi: 10.15199/48.2024.02.25.

[9] Moulichon A., Garbuio L., Debusschere V., Rahmani M. A., Hadj-Said N., A Simplified Synchronous Machine Model for Virtual Synchronous Generator Implementation, in 2019 IEEE Power & Energy Society General Meeting (PESGM), IEEE, Aug. 2019, 1–5. doi: 10.1109/PESGM40551.2019.8973392.

[10] Mouni E., Tnani S., Champenois G., Comparative study of three modelling methods of synchronous generator, in IECON 2006 - 32nd Annual Conference on IEEE Industrial Electronics, IEEE, Nov. 2006, 1551–1556. doi: 10.1109/IECON.2006.347987.

[11] Emami A., Araújo R., Cruz S., Hadla H., Aguiar A. P., A systematic approach to modeling synchronous generator using Markov parameters and Takagi–Sugeno fuzzy systems, Expert Syst. Appl., 235 (2024), 121122, doi: 10.1016/j.eswa.2023.121122.

[12] Barszcz T., Zabaryllo M., Concept of automated fault detection of large turbomachinery using Machine Learning on transient data, Diagnostyka, 20 (2018), No. 1, 63–71, doi: 10.29354/diag/100399.

[13] Racewicz S., Kutt F., Sienkiewicz Ł., Michna M., Ryndzionek R., Discrete Non-Integer Order Model of Synchronous Generator for Power Hardware In the Loop Implementation, Bull. Polish Acad. Sci. Tech. Sci., 73 (2025), No. 3, 154272–154272, doi: 10.24425/bpasts.2025.154272.
[14] Amilo D., Sadri K., Hincal E., Comparative Analysis of Caputo and Variable-Order Fractional Derivative Algorithms Across Various Applications, Int. J. Appl. Comput. Math., 11 (2025), No. 3, 80, doi: 10.1007/s40819-025-01887-w.
[15] Xu J., Gong Z., Li X., Tang S., Wang C., Lan Y., Mechanism Modeling and Analysis of Fractional-Order Synchronous Generator, Fractal Fract., 9 (2025), No. 4, 244, doi: 10.3390/fractalfract9040244.
[16] Racewicz S., Kutt F., Michna M., Sienkiewicz Ł., Comparative Study of Integer and Non-Integer Order Models of Synchronous Generator, Energies, 13 (2020), No. 17, 4416, doi: 10.3390/en13174416.
[17] Guo R., Shen W., Online state of charge and state of power co-estimation of lithium-ion batteries based on fractional-order calculus and model predictive control theory, Appl. Energy, 327 (2022), 120009, doi: 10.1016/j.apenergy.2022.120009.
[18] Zhang Q., Wei K., A comparative study of fractional-order models for supercapacitors in electric vehicles, Int. J. Electrochem. Sci., 19 (2024), No. 1, 100441, doi: 10.1016/j.ijoes.2023.100441.
[19] Tamani J., Radolo L., Cirrincione M., Mehta U., Mohammadi A., Modelling of an Optimized Polymer Electrolyte Membrane Fuel Cell (PEMFC) Using Fractional-Order, in 2023 IEEE International Conference on Advanced Systems and Emergent Technologies (IC_ASET), IEEE, Apr. 2023, 1–5. doi: 10.1109/IC_ASET58101.2023.10151016.
[20] Oprzędkiewicz K., Modelowanie systemów dynamicznych z wykorzystaniem transmitancji hybrydowych niecałkowitego rzędu, Przegląd Elektrotechniczny, 1 (2017), No. 6, 97–102, doi: 10.15199/48.2017.06.23.
[21] Larnene Y. A., Ladaci S., Belmeguenai A., Fractional-order model-based robust identification for a vehicle semi-active electro-rheological suspension system, Int. J. Adv. Mechatron. Syst., 11 (2024), No. 2, 111–119, doi: 10.1504/IJAMECHS.2024.139173.
[22] Dinesh T., Design of an ORBP-based fractional order controller for load frequency control in a multi-area power system with integration of RES, Przegląd Elektrotechniczny, 1 (2024), No. 9, 102–107, doi: 10.15199/48.2024.09.17.
[23] IEEEStd115, IEEE Guide: Test Procedures for Synchronous Machines Part I– Acceptance and Performance Testing Part II-Test Procedures and Parameter Determination for Dynamic Analysis, IEEE Std 115, (2010), 1–0, doi: 10.1109/IEEESTD.2010.5465885.
[24] Racewicz S., Riu D. M., Retiere N. M., Chrzan P. J., Half-Order Modeling of Saturated Synchronous Machine, IEEE Trans. Ind. Electron., 61 (2014), No. 10, 5241–5248, doi: 10.1109/TIE.2014.2301741.
[25] Racewicz S., Chrzan P. J., Riu D. M., Retiere N. M., Time domain simulations of synchronous generator modelled by half-order system, in IECON Proceedings (Industrial Electronics Conference), 2012, 2074–2079. doi: 10.1109/IECON.2012.6388739.
[26] Kundur P., Power System Stability and Control - Prabha Kundur - McGraw-Hill Education, 1994.
[27] Racewicz S., Riu D. M., Retière N. M., Chrzan P. J., Half-order modelling of turboalternators – An adapted method of parameter identification, in International Conference on Electrical Machines ICEM 2006, Chania, Crete Island, 2006, 1–6.